Molecular Dynamics Simulation of a Phenylene Polymer. 1. Poly(phenylene oxide)

C. L. Chen,* H. L. Chen, C. L. Lee, and J. H. Shih

Department of Chemistry, National Sun Yat-sen University, Kaohsiung, Taiwan 80424, ROC

Received September 15, 1993; Revised Manuscript Received November 24, 1993•

ABSTRACT: A molecular dynamics (MD) simulation of a simple phenylene polymer, poly(phenylene oxide) (PPO), was carried out with the TRIPOS 5.2 force field. Two types of molecular motion were examined: rotation of individual phenylene rings and torsion of a larger segment (i.e., a four-oxygen segment (FOS)) involving four ether oxygen atoms and three phenylene rings. Model compounds, diphenyl ether and 1,4-bis(4-phenoxyphenoxy)benzene, were used to help the analysis of the results. Based on the trajectory analysis, "in-phase" cooperative rotations of neighboring phenylene rings and "out-of-phase" cooperative rotations of consecutive FOS's superimposed on random segmental wiggles, were observed. Packing effects were found to be important for the larger FOS rotations but not for the rotation of individual rings. The diffusion coefficient for the torsion of an FOS is about half of that for the rotation of an individual phenylene ring but remains within the same order of magnitude.

Introduction

The mobility of phenylene rings as well as larger segments in phenylene polymers has been the subject of many studies. Experimentally, a variety of techniques including dynamic mechanical spectroscopy,[1-4] dielectric spectroscopy,[5,6] and solid-state nuclear magnetic resonance spectroscopy (NMR)[7-13] have been applied to explore molecular motions in this particular kind of polymer. In the study of Bisphenol A polycarbonate (BPAPC), experimental evidence suggests that the rotational motions of the phenylene rings should be closely related to the molecular origin of its mechanical toughness. As for the case of semicrystalline poly(oxy-1,4-phenyleneoxy-1,4-phenylenecarbonyl-1,4-phenylene) (PEEK), evidence indicates a higher segmental mobility of chains in the amorphous phase state.

In addition to experimental effects, theoretical calculations may serve to assist in the identification of the sources of the possible modes of molecular motions. Examples of theoretical calculations include molecular mechanics[13-17] and quantum mechanical calculations.[18-21] Sung et al. have used CNDO/2 (complete neglect of differential overlap) to study the rotations of phenylene rings in BPAPC and its derivative tetramethyl-Bisphenol A polycarbonate (TMPC).[18,19] Consistent with previous NMR results,[8,9] various kinds of motions of phenylene rings, including small-amplitude oscillations, 180° flips, and synchronous rotations, were identified. In the study of TMPC, Sung et al. found that segmental motions are energetically more resisted.[19] This was explained in terms of a molecular model proposed earlier by Jones.[21] In a CNDO/2 study of PEEK, Chen et al. proposed crankshaft types of molecular motions involving three consecutive phenylene rings.[20] One drawback of these computational studies is that they are based on small isolated analogue compounds lacking precise accounting of packing effects and the segments may be too small to represent a polymer chain.

In the present article, we report our MD simulation results of poly(phenylene oxide) (PPO) in its amorphous state. The advantage of MD is that both dynamic and statistical properties of a large complicated system can be simulated. The repeating unit of PPO contains one phenylene ring and an ether oxygen atom and is the simplest real phenylene polymer. The simplicity of PPO simplies the analysis of molecular motions. This simulation is our preliminary attempt to study the dynamics of molecular motion in phenylene polymers.[18-20] Additional work on a closely related polymer, PEEK, is in progress.

Method

The TRIPOS 5.2 force field[22] was adopted to carry out the MD simulation. The potential can be expressed as

$$V = V_{vdw} + V_s + V_b + V_t + V_{pl}$$

$$V_{vdw} = k_{vdw}(1.0/a^{12} - 2.0/a^6)$$

$$V_s = k_s(l - l_0)^2$$

$$V_b = k_b(\Theta - \Theta_0)^2$$

$$V_t = k_t(1 + (s/|s|)\cos(|s|B))$$

$$V_{pl} = k_{pl}d^2$$

where V_{vdw} is the van der Waals potential, V_s is the bond stretch potential, V_b is the angle bending potential, V_t is the torsional potential, V_{pl} is the out-of-plane bending potential, k represents the corresponding force constant, a is the distance between the two atoms divided by the sum of their radii, l represents the bond length, Θ represents the bending angle (with subscript zero indicating the equilibrium value), B is the torsional angle, s is a constant specific to each torsional element, and d is the distance from the atom to the plane defined by its attached atoms. The parameters used in the present simulation are adopted from ref 22. The reason for chosing this force field was based on its simplicity and accuracy.

The MD simulation was carried out on a CONVEX C3840 computer. Our PPO chain contains 63 repeating units and one phenylene ring at the end. The system was prepared by the following procedure. Initially, a single PPO chain was put into a big cubic box with the box dimensions much larger than the chain size of the polymer. The system was allowed to "equilibrate" until the kinetic

* To whom correspondence should be sent.
• Abstract published in *Advance ACS Abstracts,* March 1, 1994.

0024-9297/94/2227-2087$04.50/0 © 1994 American Chemical Society

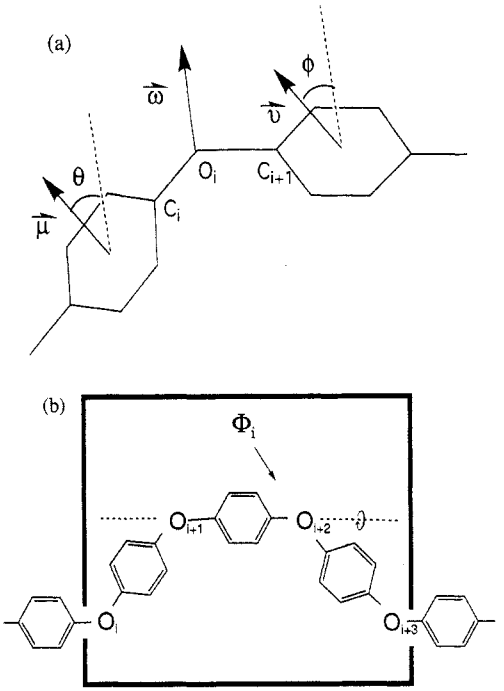

Figure 1. Definitions for (a) paired dihedral angles, (θ,ϕ), of adjacent phenylene rings and (b) torsional angle Φ of four-oxygen segment.

energy of the system was fluctuating within a predetermined range around $3Nk_BT/2$. N is the total number of atoms in the system, k_B is the Boltzmann constant, and T is the absolute temperature. The size of the box was then reduced slightly, and the system was again allowed to equilibrate. This process was repeated until the density of the system matched its experimental value, 1.27 g/cm^3.[23] The purpose of this procedure is to avoid overcrowding of the system at the starting point of the MD run.

The temperature of our system is chosen at 300 K, which is lower than the glass transition temperature (T_g) of PPO (85 °C[23]). The Beeman algorithm[24] was used in the MD simulation to increase the speed in the integration of the equation of motion. A cutoff distance of 10 Å and periodic boundary condition were selected. A relatively small time step, 0.2 fs, was used in the simulation because of the fast vibration of the CH bond. After the system was equilibrated, 40-ps trajectories were recorded and analyzed. Although only one PPO chain was initially selected, due to the periodic boundary condition and minimum image convention, the system is essentially multichain in nature and includes the interchain interactions.

Results and Discussion

In our PPO chain, phenylene rings are numbered from 1 to 64 and the ether oxygen atoms are numbered from 1 to 63 from one end to the other. The paired dihedral angles, (θ,ϕ), of adjacent phenylene rings are defined in Figure 1a. Vector ω is normal to the C_i–O_i–C_{i+1} plane, vector μ is normal to the plane of the ith phenylene ring, and vector ν is normal to the plane of the $(i+1)$th phenylene ring. θ and ϕ are the dihedral angles between μ and ω and between ν and ω, respectively. Figure 1b defines the torsional angle, Φ, of a four-oxygen segment (FOS). The FOS consists of four oxygen atoms and three phenylene rings in between. In total, the PPO chain has 63 pairs of (θ,ϕ) and 60 Φ's.

The cooperation of rotations of adjacent phenylene rings can be visualized from the trajectories of paired dihedral angles (θ,ϕ). Given in Figure 2 are the trajectories of the 40th (θ,ϕ). In the figure, θ and ϕ change simultaneously

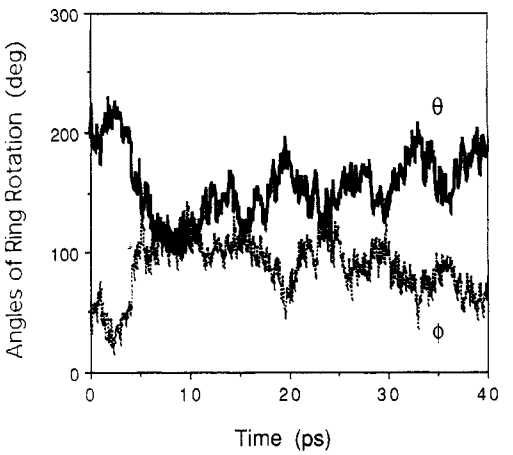

Figure 2. Trajectories of the 40th paired dihedral angles, θ (solid line) and ϕ (dotted line).

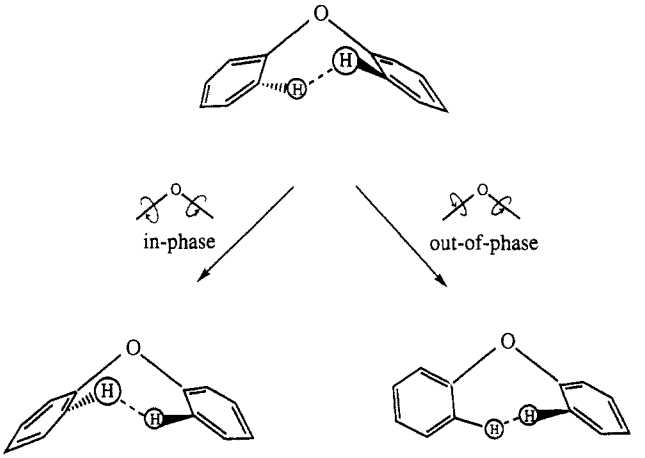

Figure 3. Illustration of "in-phase" and "out-of-phase" cooperative ring rotations.

within the given time period. This corresponds to rings rotating in the same direction; hence, it is an "in-phase" cooperative ring rotation. In the figure, a large-amplitude in-phase rotation (in excess of ca. 120°) happened within 10 ps, and two moderate-amplitude in-phase rotations (ca. 60°) happened after 10 ps. The analysis of the trajectories of (θ,ϕ) for paired phenylene rings gives 7 large-amplitude and 31 moderate-amplitude in-phase rotations. No significant "out-of-phase" cooperative ring rotations were found. The results indicate that in-phase cooperative ring rotation exists commonly in the amorphous PPO. Figure 3 shows the difference between in-phase and out-of-phase cooperative ring rotations. In the in-phase rotations, the interatomic distances of ortho hydrogens on the paired rings are approximately the same, while in the out-of-phase rotations, the interatomic distance of two ortho hydrogens on different rings decreases along the rotations. Therefore, due to the repulsion between ortho hydrogens, the out-of-phase rotations should be much more restricted than in-phase rotations. The small-amplitude cooperative ring rotations (ca. 30°) are not analyzed because it is difficult to distinguish them from the stochastic thermal oscillations of the rings.

Figure 4 compares the Φ trajectories of the 30th and the 31st FOS's. It illustrates an out-of-phase moderate-amplitude cooperative rotation (ca. 60°) of the two consecutive FOS's. The two Φ's change simultaneously in opposite directions within the given time interval. The analysis of trajectories of all Φ's gives 23 such rotations in the PPO chain. Neither large-amplitude (ca. 120°) nor in-phase moderate cooperative rotation was found. The results indicate that moderate-amplitude cooperative FOS

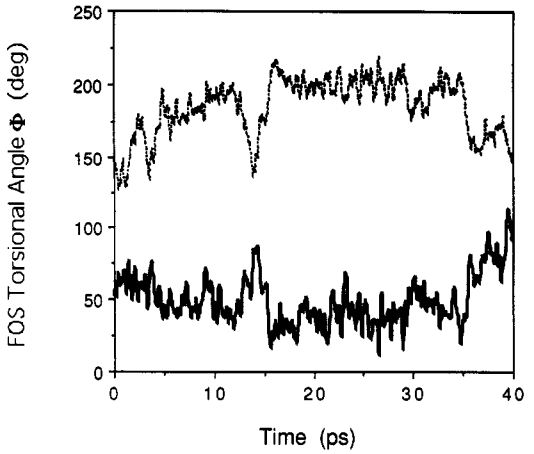

Figure 4. Φ trajectories of the 30th (solid line) and the 31st (dotted line) FOS.

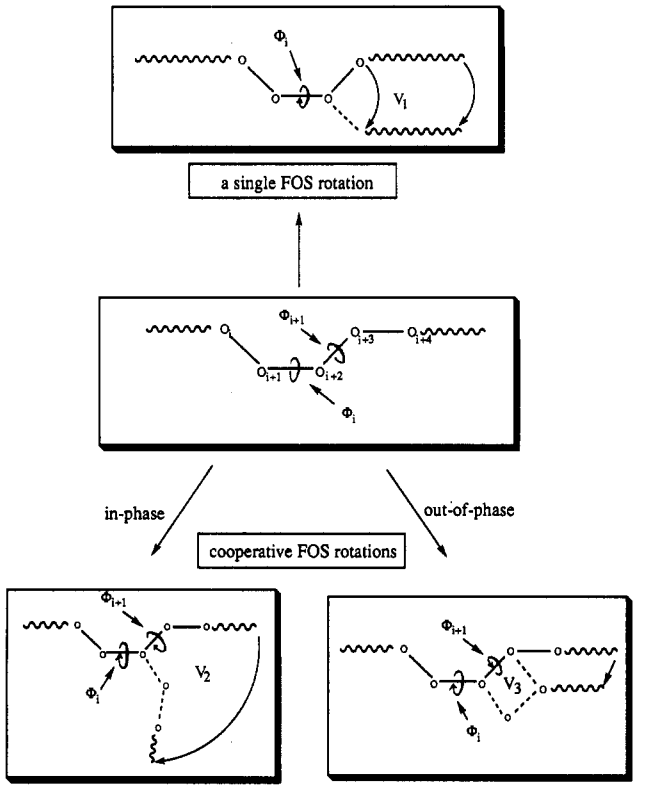

Figure 5. Spatial requirement in single and cooperative FOS.

rotations exist in the backbone of PPO. This cooperative FOS rotation is less frequent and is smaller in amplitude than cooperative ring rotations. This should be related to the larger space (free volume) required for the FOS rotations. Figure 5 shows the volume involved with various FOS rotations. Φ_i and Φ_{i+1} denote two consecutive torsional angles which consist of five oxygen atoms. If only Φ_i changes, the tail of O_{i+3} will sweep through a wide spatial volume V_1. For the in-phase motion, O_{i+3} and O_{i+4} move in the same direction, and the tail of O_{i+4} will sweep a large volume V_2. For the out-of-phase motion, O_{i+3} and O_{i+4} move in opposite directions, and the tail of O_{i+4} does not rotate. This motion will only involve the small volume V_3. Therefore, based on the requirement of free volume, the out-of-phase cooperative rotations of consecutive FOS's should be easier than in-phase rotations.

Given in Figure 6a is the conformational potential energy surface of the diphenyl ether (DPE) molecule. This model compound was selected to compare the rotations of the phenylene rings with PPO. In the figure, energies were calculated by use of the TRIPOS force field. The

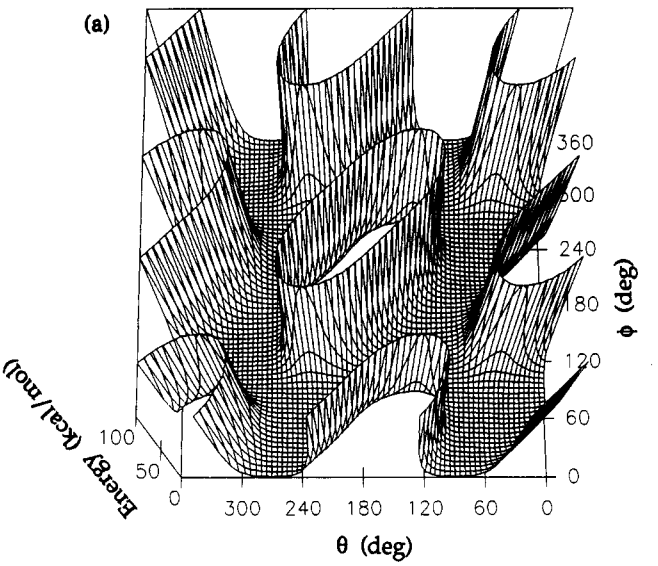

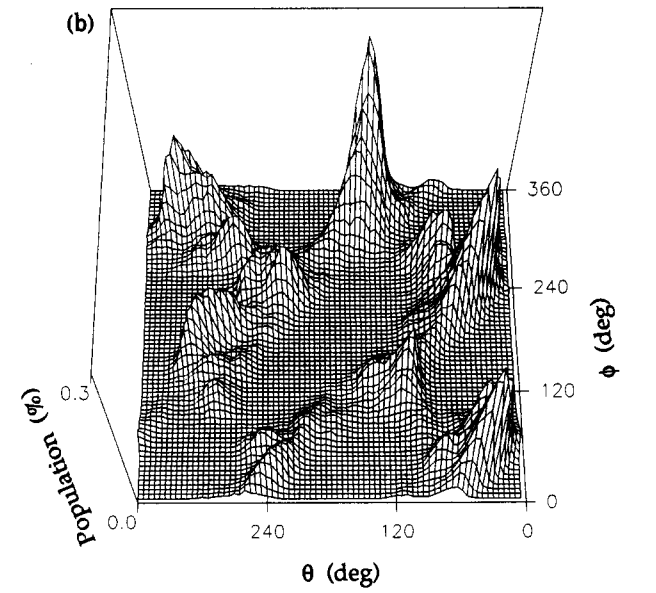

Figure 6. (a) Conformational potential energy surface of DPE evaluated with the TRIPOS force field. (b) Statistics of (θ,ϕ)'s of the PPO chain from MD simulation.

molecular geometry was fixed but the dihedral angles of the phenylene rings were allowed to vary. The equilibrium structure of the phenylene ring in the TRIPOS field was used while the ether angle and the C–O bond lengths were adopted from the corresponding MD average values in the PPO chain. The average ether angle is 113° and the C–O bond length is 1.395 Å. Given in Figure 6b are the statistics of the (θ,ϕ)'s of the PPO chain from MD simulation. It shows that the (θ,ϕ)'s only populate the low-energy region in Figure 6a. This similarity in features of rotations of paired phenylene rings in PPO and DPE suggests that intermolecular interactions only slightly affect the local rotations of phenylene rings in amorphous PPO chains.

Given in Figure 7 is the conformational potential energy curve of the compound 1,4-bis(4-phenoxyphenoxy)benzene (BPPB). The torsional angle of the oxygen backbone of BPPB, φ, is the analogue of Φ (torsional angle of the FOS) in the PPO chain. The potential energy was calculated with fixed φ at intervals of 10° from 0° to 360°, using the TRIPOS force field. During the calculation, bond lengths and bond angles in the backbone of BPPB were fixed, and other coordinates of atoms on rings were optimized by the energy minimization method of steepest descents. Figure

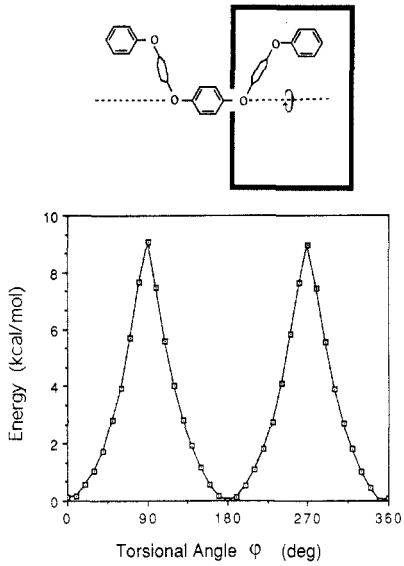

Figure 7. Conformational potential energy curve of 1,4-bis(4-phenoxyphenoxy)benzene.

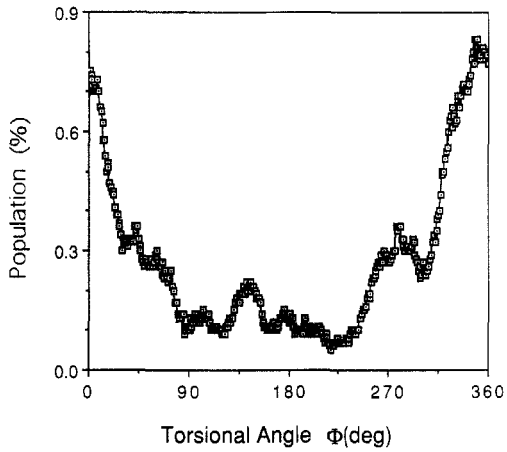

Figure 8. Population of torsional angle, Φ, of four-oxygen segments.

7 shows that the minimum-energy configuration of BPPB is at $\varphi = 0°$ (360°) or 180°. This indicates that the most stable conformation of the oxygen backbone of BPPB is the *cis* or *trans* rearrangement with a conversion barrier of ~9 kcal/mol. Given in Figure 8 is the MD stimulated population of Φ in amorphous PPO. The figure shows that the largest distribution of Φ is around 0° (or 360°); only a small population is seen in the 180° region. However, a significant population is seen in the 270° region, which corresponds to the maximum-energy conformation of BPPB. This implies that some interactions between the FOS in a PPO chain and its surroundings exist. The origins of these interactions must come from long-range interactions. It therefore appears that packing effects may indeed be important for the rotations of large segments in the amorphous PPO.

Given in Figure 9 is the simulated population of rotational angle, α, of a single phenylene ring around its average value. This was obtained by averaging all θ and ϕ values of the phenylene rings. The average amplitude is approximately ±60°. We did not find any rotation corresponding to the 180° flip of a single phenylene ring. The rotational energy barrier of the 180° ring flip was estimated as 23 kcal/mol based on results of CNDO/2 calculations.[20] The average thermal kinetic energy is only ~0.3 kcal/mol per degree of freedom in the simulation. Therefore, the possibility of 180° rotation of a phenylene ring in the present room temperature system can be

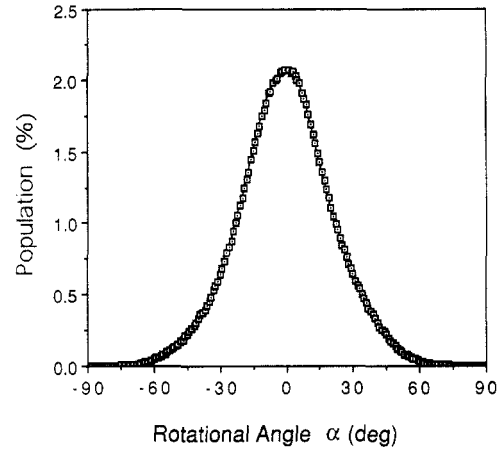

Figure 9. Population of rotational angle, α, of a single phenylene ring around its average value.

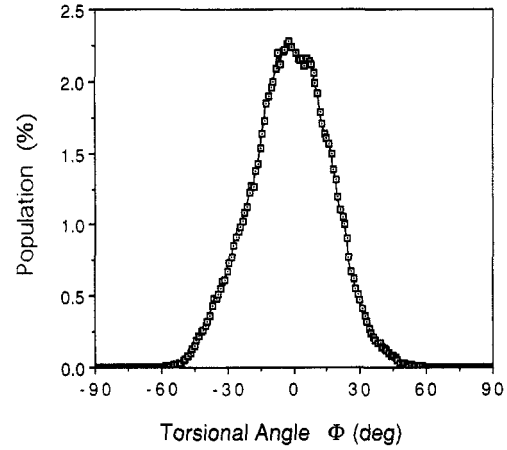

Figure 10. Population of torsional angle, Φ, of the four-oxygen segment around its average value.

neglected statistically. Given in Figure 10 is the simulated population of Φ around its average value. The average amplitude is approximately ±45°. This amplitude is smaller than that of a single phenylene ring. This implies that the rotation of large segments is somewhat more restricted than that of rings.

To compare the mobility of individual phenylene rings with that of the FOS, rotational diffusion coefficients (D) in α and Φ are evaluated by the relationship

$$2Dt = \lim_{t\to\infty} \langle |\chi - \chi_0|^2 \rangle$$

where χ is the corresponding angle and the term in brackets denotes the mean square displacement of the angle. Given in Figure 11 are the mean square displacements of α and Φ. The diffusion coefficients of a phenylene ring and an FOS are estimated as 5.67 and 3.18 deg²/ps, respectively. This indicates that torsion of an FOS is slower than rotation of a single phenylene ring, but the rates are within the same order of magnitude. The torsional motion of an FOS, involving the movement of a significantly larger segment of the backbone, is more difficult in comparison with the rotation of an individual phenylene ring, but the effect is not extremely strong in the present case for amorphous PPO.

Conclusions

By means of MD simulation, we have analyzed rotations of phenylene rings and torsion of four-oxygen segments. In the amorphous PPO, "in-phase" cooperative ring rotations with moderate- and large-amplitude were found

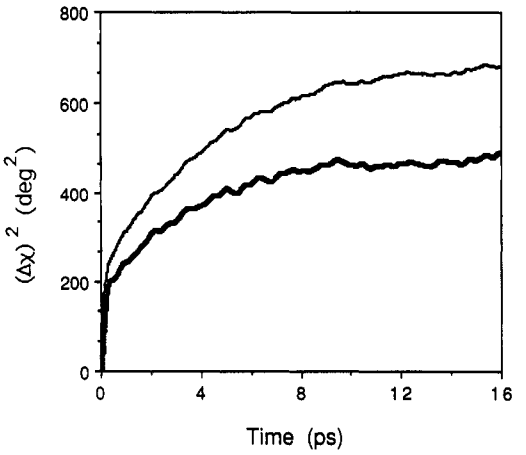

Figure 11. Mean square displacements of rotational angles of the phenylene ring (thin line) and the four-oxygen segment (heavy line).

to be quite common. "Out-of-phase" cooperative rotations of four-oxygen segments also exist but with smaller amplitudes and are less frequent. Long-range interactions are not important for ring rotations; the packing effect, however, is more important for the torsional motion of four-oxygen segments. The rotation of an individual phenylene ring is less restricted and therefore faster than the torsion of a four-oxygen segment, but only by a moderate factor of ca. 2.

One deficiency of the present work is the lack of experimental data for comparison purposes, although we feel that the present results have provided some insights into the molecular motions of phenylene polymers in general. Additional work on closely related polymers such as PEEK and PC, for which extensive NMR observations have been made, is in progress.

Acknowledgment. Thanks are due to the Computer Center of NSYSU for their help during this work. Many valuable suggestions from and discussions with Prof. A. C. Su of the Institute of Material Science and Engineering are greatly appreciated. This work is financially supported by Contract No. NSC-82-0208-M-110-026 from the National Science Council, ROC.

References and Notes

(1) Yee, F. A.; Smith, S. A. *Macromolecules* **1981**, *14*, 54.
(2) Havriliak, S., Jr.; Pogonowski, C. S. *Macromolecules* **1989**, *22*, 2466.
(3) Sasuga, T.; Hagiwara, M. *Polymer* **1985**, *26*, 501.
(4) Sasuga, T.; Hagiwara, M. *Polymer* **1986**, *27*, 821.
(5) Starkweather, H. W., Jr.; Avakian, P. *Macromolecules* **1989**, *22*, 4060.
(6) Pochan, J. M.; Pochan, D. F. *Macromolecules* **1980**, *13*, 1577.
(7) Goodwin, A. A.; Hay, J. N. *Polym. Commun.* **1989**, *30*, 288.
(8) Spiess, H. W. In *Advances in Polymer Science*; Kausch, H., Zachmann, H. G., Eds.; Springer-Verlag: Berlin, 1984; Vol. 66.
(9) Schaefer, J.; Stejskal, E. O.; McKay, R. A.; Dixon, W. T. *Macromolecules* **1984**, *17*, 1479.
(10) Roy, A. K.; Jones, A. A.; Inglefield, P. T. *Macromolecules* **1981**, *14*, 64.
(11) Henriches, P. M.; Luss, H. R. *Macromolecules* **1988**, *21*, 860.
(12) Walton, J. H.; Lizak, M. J.; Conradi, M. S.; Gullion, T.; Schaefer, J. *Macromolecules* **1990**, *23*, 415.
(13) Clark, J. N.; Jagannathan, N. R.; Herring, F. G. *Polymer* **1988**, *29*, 341.
(14) Poliks, M. D.; Schaefer, J. *Macromolecules* **1990**, *23*, 1941.
(15) Tonelli, A. E. *Macromolecules* **1972**, *5*, 558.
(16) Cowie, J. M.; Ferguson, R. *Polymer* **1987**, *28*, 503.
(17) Heijboer, J.; Baas, J. M. A.; van de Graaf, B.; Hoefnagel, M. A. *Polymer* **1987**, *8*, 509.
(18) Sung, Y. J.; Chen, C. L.; Su, A. C. *Macromolecules* **1990**, *23*, 1941.
(19) Sung, Y. J.; Chen, C. L.; Su, A. C. *Macromolecules* **1991**, *24*, 6123.
(20) Chen, C. L.; Chang, J. L.; Su, A. C. *Macromolecules* **1992**, *25*, 1941.
(21) Jones, A. A. *Macromolecules* **1985**, *18*, 902.
(22) Clark, M.; Cramer, R. D., III; Van Opdenbosch, N. *J. Comput. Chem.* **1989**, *10*, 982.
(23) Dawson, P. C.; Blundell, D. J. *Polymer* **1980**, *21*, 577.
(24) Beeman, D. *J. Comput. Phys.* **1976**, *20*, 130.